Electrodeposition of Zinc-SiO2 composite

Kazuo Kondo
Okayama University

Atsufumi Ohgishi
Okayama University

Zennosuke Tanaka
Okayama University

Journal of The Electrochemical Society, **147** (7) 2611-2613 (2000)
S0013-4651(99)12-094-9 CCC: $7.00 © The Electrochemical Society, Inc.

Electrodeposition of Zinc-SiO_2 Composite

Kazuo Kondo,*,z Atsufumi Ohgishi, and Zennosuke Tanaka

Faculty of Engineering, University of Okayama, 3-1-1 Tsushima-Naka, Okayama 700-0082, Japan

The incorporation mechanism of SiO_2 particles into zinc electrodeposit is discussed. The SiO_2 particles precipitate in two ways on the $(00{\cdot}1)_\eta$ of zinc electrodeposit: by lined up particles along the laterally growing macrosteps on the $(00{\cdot}1)_\eta$ and by randomly dispersed particles on the $(00{\cdot}1)_\eta$. These particles incorporate into the electrodeposits by following two processes. The sidewalls of particles are incorporated into the macrosteps at the edge of $(00{\cdot}1)_\eta$. The bottom of randomly dispersed particles are incorporated into the $(00{\cdot}1)_\eta$ probably by the atomic steps.

Manuscript submitted December 27, 1999; revised manuscript received March 30, 2000.

Zinc and zinc alloy electrodeposited steel sheets have been used for automobile bodies due to their high corrosion resistance. Zinc electrodeposit composite with SiO_2 or Al_2O_3 particles is known to show good corrosion resistance and paint ability. For example, Hiramatsu *et al.*[1,2] have reported an improvement in corrosion resistance and paint ability of zinc electrodeposit composite with SiO_2 particles treated with silane coupling. Aslanidis *et al.*[3] also have reported an improvement in corrosion resistance and paint ability of zinc electrodeposit if the SiO_2 particle surfaces were covered with titania. Guglielmi[4] reported the two-step absorption mechanism of the composite particles. The inclusion process of the composite particles is important for understanding the adhesion mechanism between the electrodeposit and painted film. No report so far has been published on this inclusion process.

The author, K.K., has reported on the crystal growth of zinc and zinc alloy electrodeposits.[5-8] The hexagonal columnar crystals are composed of the hexagonal plates thin in the *c* axis direction. By atomic force microscopy (AFM) studies, the author reported the growth on the hexagonal plates of these hexagonal columnar crystals.[9-11] The $(00{\cdot}1)_\eta$ of pure zinc electrodeposit consists of numerous 30 nm granular crystals and the alignments of these granular crystals form macrosteps.[9] For the zinc-iron electrodeposit, the $(00{\cdot}1)_\eta$ consists of fish scale crystals and the edges of these fish scale crystals are the macrosteps.[10] For the zinc-nickel electrodeposit, the $(00{\cdot}1)_\eta$ also consists of fish scale crystals, which are the edges of hexagonal plates. The macrostep heights of the hexagonal plates are 3 nm, which corresponds to about 20 zinc atoms.[11]

Zinc and zinc alloy electrodeposits grow with the lateral macrosteps on the $(00{\cdot}1)_\eta$ of hexagonal columnar crystals. In this report, the incorporation mechanism of SiO_2 particles into these lateral zinc macro steps is discussed.

Experimental

Table I shows the bath composition. The concentration of $ZnSO_4$ was 1.4×10^3 mol m^{-3} and that of Na_2SO_4 was 0.53×10^3 mol m^{-3}. Additive of 2.81×10^{-3} mol m^{-3} of Sn^{2+} and 0.3×10^3 g m^{-3} of colloidal silica (Snowtex-OL from Nissan Chemical Industrial, Ltd.) were added. Table II lists the condition for the electrodeposition. The current density was 3000 A m^{-2}. The bath temperature was kept at 323 K at 2.0 pH. The bath was agitated by a stirrer with string rate of 13.3 rps. The substrate was a commercial low carbon steel 0.8 mm thick. Prior to electrodeposition, the cathode was degreased in acetone with ultrasonic cleaning for 15 min, pickled with 10 vol % sulfuric acid, and rinsed in deionized water. The platinum anode was located 10 mm apart from the cathode. The deposition time was 10 s.

The morphology of deposits was examined by scanning electron microscopy (SEM, Hitachi S-4500) and AFM (Digital Instruments Nano Scope III). The AFM was operated in contact mode using a single-crystal cantilever of Si_3N_4 (NP-S). The crystal structure was analyzed by X-ray diffraction (XRD, Rigaku RAD-2VC) of 40 kV and 30 mA.

* Electrochemical Society Active Member.
z E-mail: kkondo@cc.okayama-u.ac.jp

Table I. Bath composition

	Concentrations
$ZnSO_4$	1.4×10^3 mol m^{-3}
Na_2SO_4	0.53×10^3 mol m^{-3}
$SnSO_4$	2.81×10^{-3} mol m^{-3}
SiO_2	0.3×10^3 g m^{-3}

Table II. Condition for the electrodeposition.

Stirring rate	13.3 rps
pH	2.0
Bath temperature	323 K
Current density	3000 A m^{-2}
Deposit time	10 s

Results

SEM observation and XRD.—Figure 1 is the top SEM view of zinc-SiO_2 composite electrodeposit with Sn^{2+} as additive. The hexagonal plane crystals of about 1.0 μm diam become parallel to the substrate. The SiO_2 particles of about 50 nm diam white particles precipitate on these hexagonal plane crystals.

These SiO_2 particles precipitate in two ways on this plane. The one is lined up particles along a macrostep (Fig. 1, larger arrow). The other is randomly dispersed SiO_2 particles on the plane. These hexagonal plane crystals form hexagonal columnar crystals.[5-8] At the edge of these hexagonal columnar crystals, the hexagonal plane crystals form a layer-by-layer stacking.

Figure 2 is the result of XRD of this zinc-SiO_2 composite electrodeposit. The $(00{\cdot}2)_\eta$ diffraction has the strongest intensity. This strongest intensity indicates that the electrodeposit has a *c* axis orientation and the hexagonal plane crystals are the $(00{\cdot}1)_\eta$ plane. The diffraction of the SiO_2 particles does not exist, since the particles are amorphous.

Magnified SEM and AFM observations.—Figure 3 is the magnified SEM micrograph along the macrostep on the $(00{\cdot}1)_\eta$. This macrostep is located close to the edges of the $(00{\cdot}1)_\eta$ plate. The SiO_2 particles line up along this macrostep and furthermore, all these particles are incorporated into the sidewall of this macrostep. These incorporated particles are also indicated with smaller arrows in Fig. 1 of the SEM top view.

Figure 4 again is an AFM image along the macrostep on the $(00{\cdot}1)_\eta$. A line is drawn on the surface plot of Fig. 4a. The section analysis along a line on the surface plot is shown in Fig. 4b. The

S0013-4651(99)12-094-9 CCC: $7.00

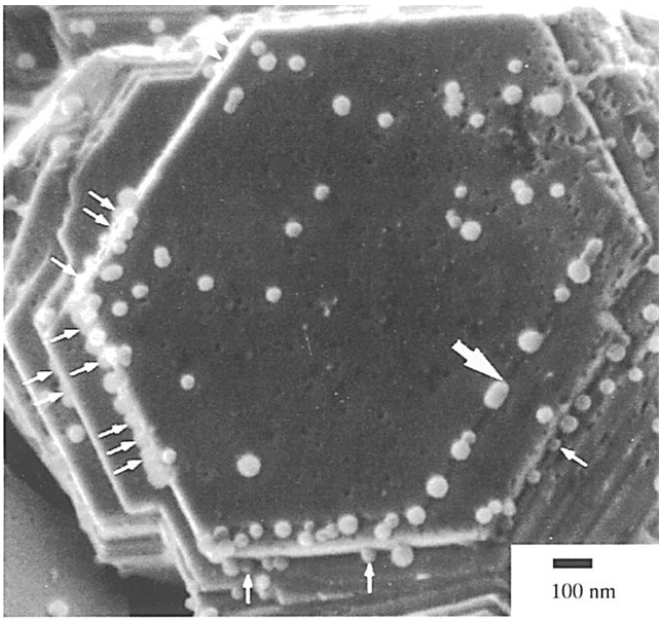

Figure 1. Top-view micrograph of zinc-SiO_2 composite electrodeposit.

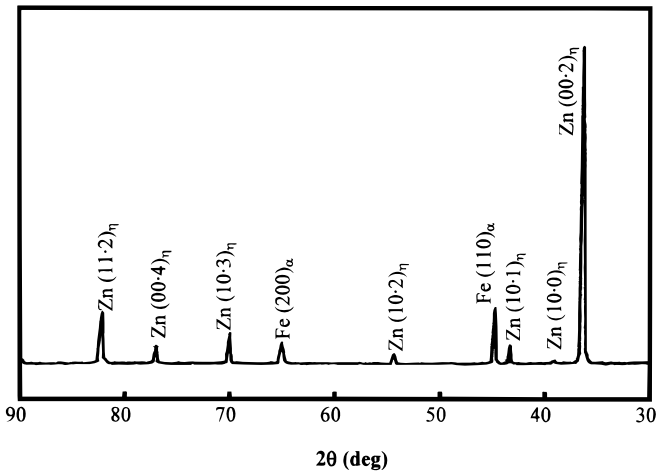

Figure 2. XRD of zinc-SiO_2 composite electrodeposit.

height difference between smaller arrows measures the SiO_2 particle diameter and that between larger arrows measures the macrostep height. The section analysis shows that the SiO_2 particles have diameter of 50 nm and the height of the macrostep which incorporates these particles is about 100 nm.

SEM observation with stage tilting.—Figure 5 is the *c* axis orientation electrodeposit with tilting the SEM stage. The micrograph shows the laterally growing macrostep on the $(00{\cdot}1)_\eta$. These SiO_2 particles precipitate in two ways, the randomly dispersed particles and the lined-up particles along the macrostep. The bottoms of the randomly dispersed particles are incorporated into the $(00{\cdot}1)_\eta$ plane (Fig. 5, arrows). The bottoms of lined-up particles along the macrosteps, however, are not incorporated into the $(00{\cdot}1)_\eta$.

Figure 6 is the fractured surface of the electrodeposit. The fractured surface shows that the SiO_2 particles are incorporated into the inside of the electrodeposit.

Discussion

The SiO_2 particles line up along the macrosteps on the $(00{\cdot}1)_\eta$ plane (Fig. 1, larger arrow). These particles start to be incorporated into the sidewalls of the macrosteps when the macrosteps reach close to the edge of the $(00{\cdot}1)_\eta$ (Fig. 1, smaller arrow, Fig. 3). These particles, at the same time, randomly disperse on the $(00{\cdot}1)_\eta$. The bottoms of these randomly dispersed particles are incorporated into the $(00{\cdot}1)_\eta$ (Fig. 5, arrows). The bottoms of the lined-up particles along

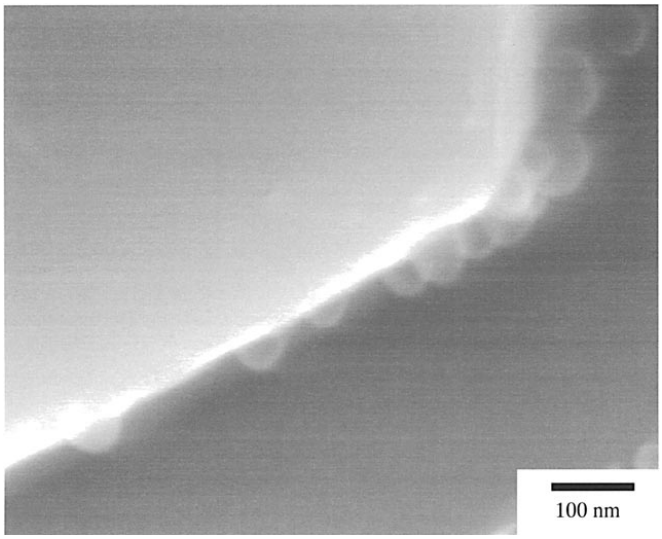

Figure 3. Top-view micrograph along macrostep of the $(00{\cdot}1)_\eta$.

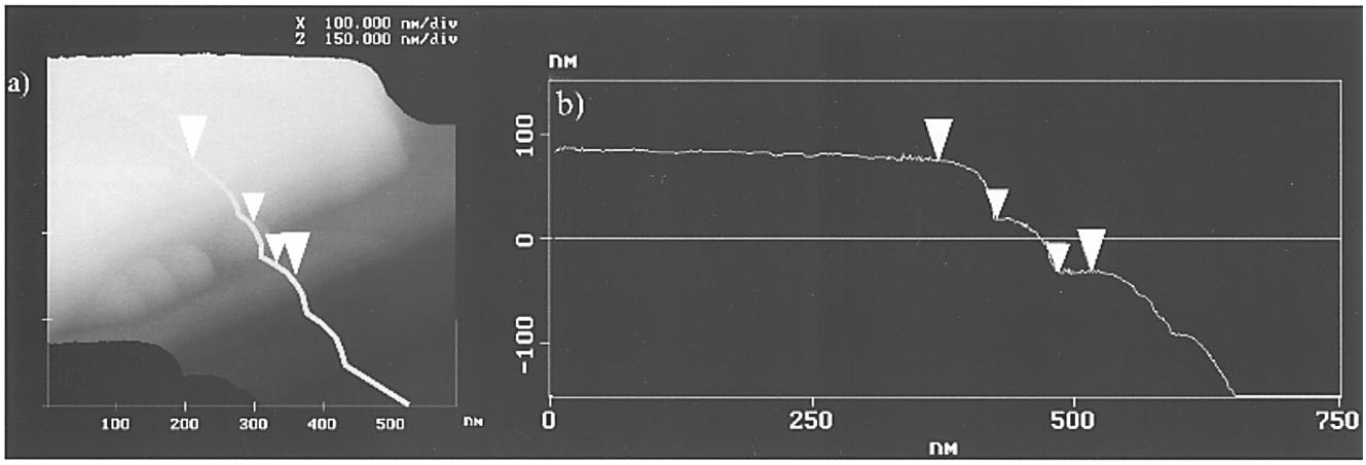

Figure 4. AFM image along the macrostep on the $(00{\cdot}1)_\eta$: (a) surface plot and (b) section analysis.

S0013-4651(99)12-094-9 CCC: $7.00

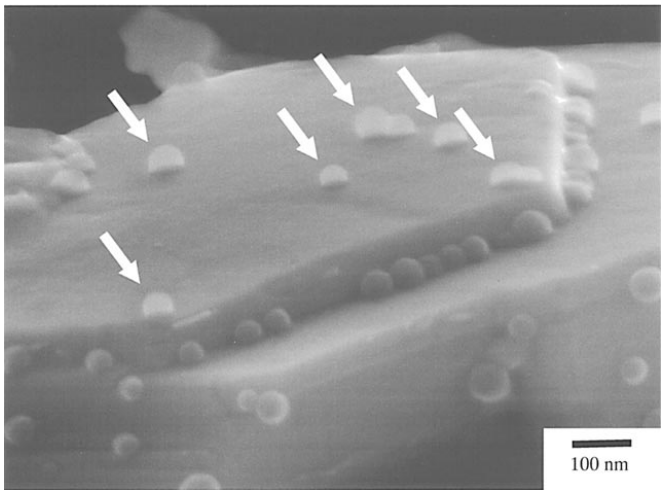

Figure 5. Side-view micrograph of zinc-SiO_2 composite electrodeposit.

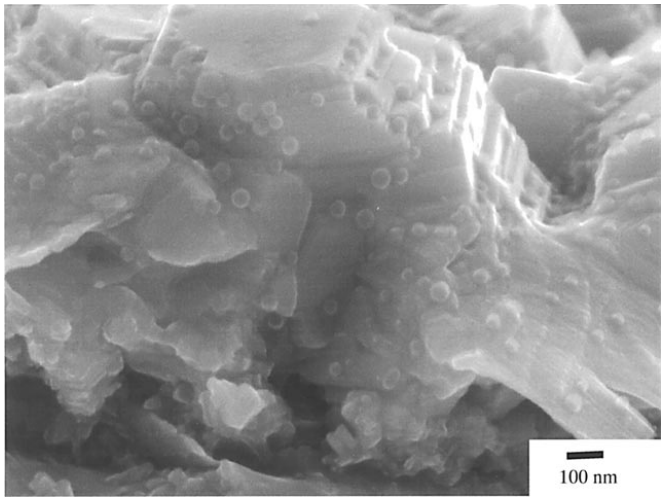

Figure 6. Fractured surface of electrodeposit.

the macrosteps, however, are not incorporated into the $(00{\cdot}1)_\eta$ (Fig. 5).

The zinc electrodeposit incorporates SiO_2 particles in two ways. The particles line up along the macrosteps. The macrosteps grow laterally and sweep up the particles to the $(00{\cdot}1)_\eta$ edge. The particles are eventually incorporated into the macrostep sidewalls at the $(00{\cdot}1)_\eta$ edge (Fig. 7). The randomly dispersed particles remain at their absorbed sites. The lower portions of these randomly dispersed particles are incorporated into the $(00{\cdot}1)_\eta$. The atomic steps are thought to incorporate these randomly dispersed particles (Fig. 7).

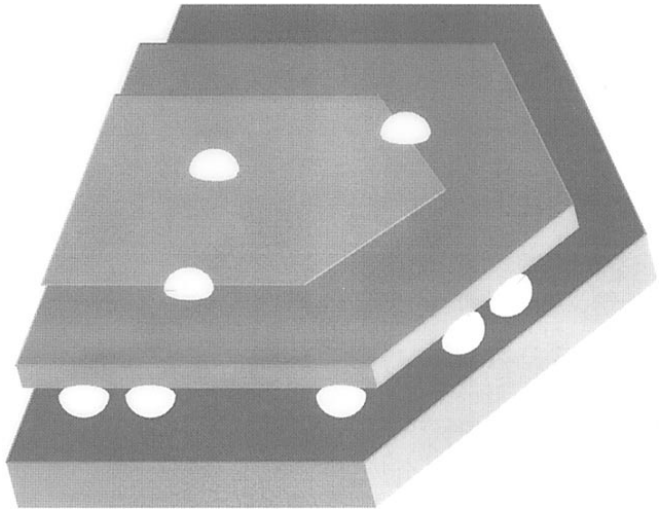

Figure 7. Incorporation mechanism.

Conclusions

The SiO_2 particles precipitate in two ways on the $(00{\cdot}1)_\eta$: by lined-up particles along the laterally growing macrosteps and by randomly dispersed SiO_2 particles on the $(00{\cdot}1)_\eta$. These particles incorporate into the electrodeposit by the following two processes.

1. The particles line up along the laterally growing macrosteps. These particles must be incorporated into the macrostep sidewalls at this edge of $(00{\cdot}1)_\eta$.
2. The randomly dispersed particles are incorporated into the $(00{\cdot}1)_\eta$ from their bottoms probably by the atomic steps.

Acknowledgments

Part of this research was supported by the Iron and Steel Institute, Japan.

The University of Okayama assisted in meeting the publication costs of this article.

References

1. M. Hiramatsu and H. Kawasaki, *Hyoumen-gijitu*, **40**, 406 (1989).
2. M. Hiramatsu, H. Kawasaki, T. Omi, and Y. Nakayama, *Hyoumen-gijitu*, **38**, 12 (1987).
3. D. Aslanidis, J. Fransaer, and J.-P. Celis, *J. Electrochem. Soc.*, **144**, 2352 (1997).
4. N. Guglielmi, *J. Electrochem. Soc.*, **119**, 1009 (1972).
5. K. Kondo, *Tetsu-to-Hagane*, **74**, 2300 (1988).
6. K. Kondo, *ISIJ Int.*, **29**, 517 (1989).
7. K. Kondo, Ph.D. Thesis, Kyoto University, Kyoto, Japan (Jan 1994).
8. K. Kondo, *Tetsu-to-Hagane*, 7**6**, 592 (1990).
9. K. Kondo, T. Murakami, F. Cerwinski, and K. Shinohara, *ISIJ Int.*, **37**, 140 (1997).
10. F. Czerwinski, K. Kondo, and J. A. Szpunar, *J. Electrochem. Soc.*, **144**, 481 (1997).
11. K. Kondo and Z. Tanaka, *ISIJ Int.*, **38**, 778 (1998).